Chromium as resonant donor impurity in PbTe

M. D. Nielsen,[1] E. M. Levin,[2] C. M. Jaworski,[1] K. Schmidt-Rohr,[2] and J. P. Heremans[1,3,*]

[1]*Department of Mechanical and Aerospace Engineering, The Ohio State University, Columbus, Ohio 43210-1142, USA*

[2]*Division of Materials Sciences and Engineering, Ames Laboratory US DOE, Iowa State University, Ames, Iowa, 50011, USA*

[3]*Department of Physics, The Ohio State University, Columbus, Ohio, 43210, USA*

(Received 25 November 2011; published 25 January 2012)

We synthesize and perform structural, thermoelectric, magnetic, and ^{125}Te NMR characterization measurements on chromium-doped PbTe. ^{125}Te NMR and magnetic measurements show that $Pb_{1-x}Cr_xTe$ is a solid solution up to $x = 0.4$ at.% and forms an n-type dilute paramagnetic semiconductor. The Cr level is resonant and pins the Fermi level about 100 meV into the conduction band at liquid nitrogen temperatures and below, but it moves into the gap as the temperature increases to 300 K. ^{125}Te NMR spectra exhibit a Knight shift that correlates well with Hall effect measurements and resolve peaks of Te near Cr. Magnetic behavior indicates that Cr exists mainly as Cr^{2+}. No departure from the Pisarenko relation for PbTe is observed. Secondary Cr_2Te_3 and $Cr_{3+\delta}Te_4$ phases are present in samples with $x > 0.4\%$.

DOI: 10.1103/PhysRevB.85.045210 PACS number(s): 71.55.Ht, 72.20.−i, 75.20.Ck, 76.60.−k

I. INTRODUCTION

The resonant acceptor impurity Tl is known to increase the thermoelectric figure of merit zT of PbTe at high temperature.[1,2] A material's figure of merit is the parameter that dominates its efficiency in solid-state energy conversion; it is given by $zT = S^2\sigma T/\kappa$, where S is the Seebeck coefficient or thermopower, σ ($= 1/\rho$) the electrical conductivity (resistivity), and κ the thermal conductivity. Consequently, other dopants were sought that could act as resonant levels,[3–5] and in particular in the conduction band of PbTe. It was suggested very recently[6] that n-type PbTe double-doped with both chromium and iodine displays a strong increase in thermopower at temperatures starting at 400 K and reaching 600 K, leading to a power factor $S^2\sigma$ peaking above 55 μW cm^{-1}K^{-2} near 500 K, an enormous number for PbTe. Previously, chromium had been reported to form a resonant level 100 meV above the conduction band minimum of PbTe:Cr at low temperature and to exhibit Fermi level pinning;[7–10] its effect in PbTe:{Sn,Cr} has also been investigated recently.[11] The purpose of this investigation is to determine if the electrons on Cr are sufficiently delocalized to effectively increase thermopower and effective mass, as has been shown necessary for it to boost the high-temperature thermoelectric performance by contrasting the behavior of PbTe:Tl[2] with that of PbTe:Ti.[12] We also attempted to reproduce the result of Paul *et al.* on double-doped PbTe:(Cr+I), but failed.[6] Here we present a comprehensive set of complementary measurements of thermomagnetic transport and magnetic properties, augmented by ^{125}Te NMR, to identify the activity of the Cr-donor in PbTe.

II. SAMPLE PREPARATION

Ingots of $Pb_{1-x}Cr_xTe$ alloy were synthesized by loading stoichiometric amounts of pure elements (Cr in powder form) of 99.999% purity or greater into fused quartz ampoules that were sealed under a pressure less than 10^{-6} torr. The samples were heated above the melting point of PbTe, cooled through the liquidus, and subsequently annealed until x-ray peak widths reached instrumental broadening and positions were at the nominal value, indicating that residual stresses were relieved. Powder x-ray diffraction of the samples confirms a rocksalt structure. The samples were cut with a diamond wire saw into parallelepipeds approximately 1.5 × 1.5 × 6 mm^3 for the transport measurements. Irregular lumps were used for magnetic measurements; for x-ray diffraction and ^{125}Te NMR, we powdered a piece of the bulk samples.

III. TRANSPORT PROPERTIES

All transport properties were measured on the same parallelepipeds in a conventional liquid nitrogen-cooled flow cryostat. We stepped temperature from 80–400 K, the magnetic field from −15 to +15 kOe, and took steady state measurements. The Hall coefficient (R_H) of the sample with $x = 0.25\%$ was also measured in a Quantum Design PPMS down to 2 K. We report here on four transport properties; electrical resistivity (ρ) and R_H were measured using an AC bridge while thermopower (or Seebeck coefficient S) and adiabatic transverse Nernst-Ettingshausen coefficient ("Nernst" or N) were measured using the static heater and sink method. We measured the temperature gradients for S with two copper-constantan thermocouples of 0.025 mm diameter. The diameters of the wires were kept small to minimize their heat draining capability. The effect of a 15-kOe magnetic field on the sensitivity of the thermocouples was calibrated on a nonconductive, nonmagnetic standard to be 2.6% at 77 K and 2.2% at 300 K; no numerical correction was applied for this. The copper leads of the type-T thermocouples are used to measure the Seebeck voltage, and we estimate the error on this measurement to be 3%. Electrical resistivity was taken using an AC 4-wire measurement, and the main errors in this property are estimated to be 10% due to inaccuracies in measurement of sample geometry. R_H and N were measured with transverse copper leads, and we estimate the error in N to be 5%, in R_H, 7 to 10%. We applied the standard correction[13] to convert from adiabatic to isothermal N. Since the samples have a magnetic response (see following section), we sweep the Hall resistance and Nernst voltage over the entire −15 kOe to +15 kOe field

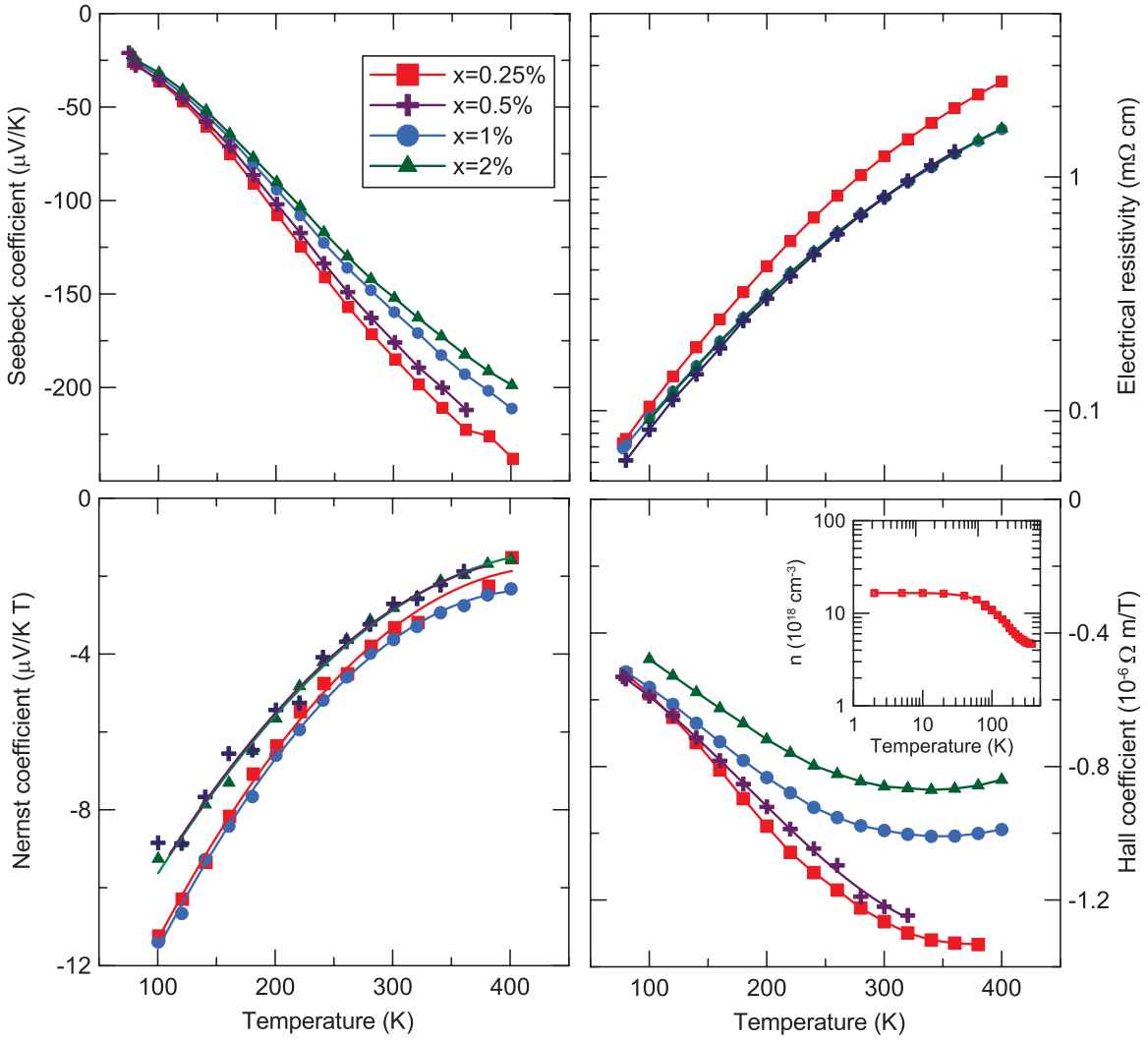

FIG. 1. (Color online) Thermopower or Seebeck coefficient, electrical resistivity, Nernst-Ettingshausen coefficient, and Hall coefficient of $Pb_{1-x}Cr_xTe$. Inset shows carrier concentration for $x = 0.25\%$. The data are shown as points; the lines are guides for the eye.

range to check for anomalous effects, but the curves remain linear in H: the Hall and Nernst coefficients (R_H and N) are then taken to be the low field slopes of the Hall resistance and Nernst voltage, respectively.

The transport coefficients S, ρ, N, and R_H from 80 K to 400 K are shown in Fig. 1. S and R_H for all samples are negative confirming that Cr is an electron donor. Electrical resistivity shows typical metallic behavior with more than an order of magnitude increase with a positive temperature coefficient. The sample with $x = 0.25\%$ has the highest ρ, which first decreases, then saturates when the amount of Cr is further increased. Increasing Cr concentration leads to a smaller R_H, or larger carrier density, at 300 K, which is reflected in a smaller thermopower. With T, R_H exhibits unique behavior: it increases in magnitude with increasing temperature in the range of 100–350 K. At $T < 80$ K and $T >$ 350 K, R_H remains relatively temperature independent. The trends in R_H correlate well with S, and we also cross-check the relation between R_H and the Knight shift in ^{125}Te NMR (see further discussion), suggesting that the change in R_H represents a change in carrier concentration and not a change in the Hall prefactor or an anomalous Hall effect. As temperature is increased, three regions of nearly linear S behavior with different slopes emerge: a low and high temperature region of S with lower slope than that of the mid-temperature range. The diminishing carrier density between 100 K and 350 K coincides with the steeper slope of S, as expected from the Mott formula. The behavior of R_H and S in relation to the Cr impurity level will be discussed quantitatively in the next paragraph. The Nernst coefficient is large, shows a similar T-dependence for all samples, and has no significantly systematic relation to Cr content.

We use the method of four coefficients[14] with the four measured transport properties (S, ρ, N, and R_H) and calculate the Fermi level relative to the bottom of the conduction band (E_F), the mobility, the density of states (DOS) or, alternatively, a DOS-effective mass (m^*), which includes the effect of the four-fold degeneracy of the conduction band pockets, and the scattering parameter (λ) defined as the exponent of the power law that characterizes the energy dependence of the relaxation time $\tau = \tau_0 E^{\lambda - 1/2}$. The parameters E_F, m^*, and λ are shown in Fig. 2 for $Pb_{1-x}Cr_xTe$. The principal result is that the Fermi

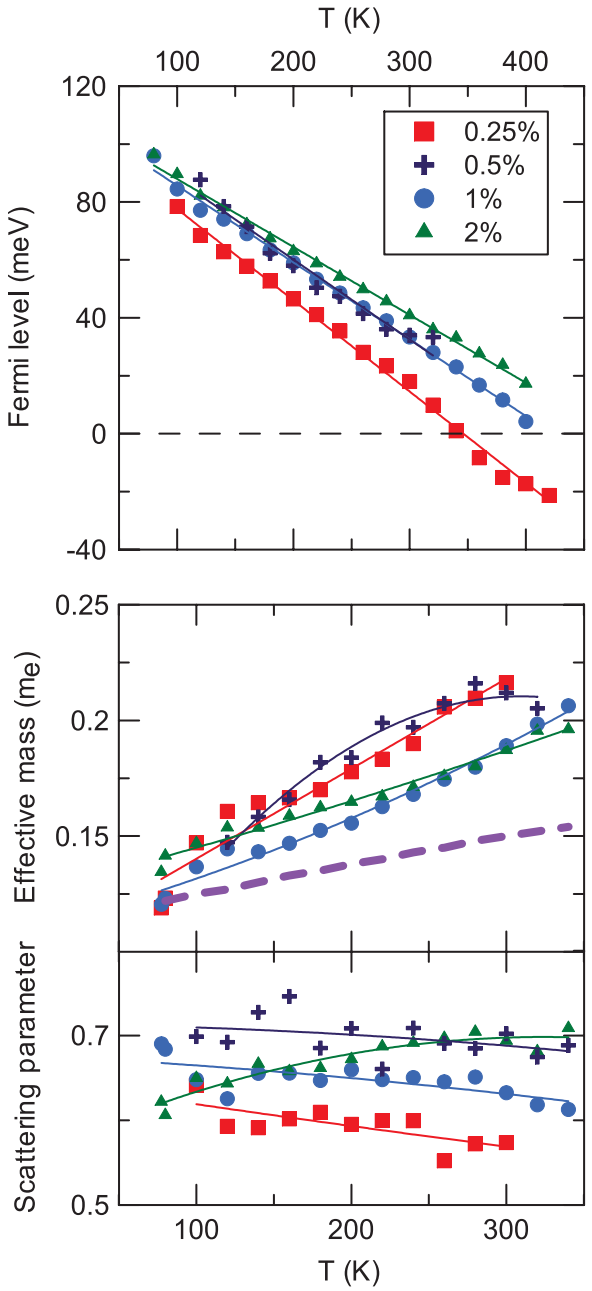

FIG. 2. (Color online) Calculated position of the Fermi level with respect to the conduction band edge, effective carrier DOS mass, and scattering parameter λ for $Pb_{1-x}Cr_xTe$. The dashed line is the DOS-mass for the conduction band of PbTe: no significant increase is observed in $Pb_{1-x}Cr_xTe$ (the ordinate axis is expanded for clarity).

level is calculated to move toward the bottom of the conduction band with increased temperature. Indeed, for $x = 0.25\%$ the Fermi level actually moves into the band gap around 350 K with a linear temperature dependence of 0.31 meV K^{-1}. The slope of the $E_F(T)$ is somewhat less steep at higher x, -0.23 meV K^{-1} for $x = 2\%$. This explains the flattening of the Hall coefficient at $T > 300$ K. Assuming that the Cr level indeed pins E_F, then the conclusion is that the Cr impurity level moves toward the conduction band edge with increasing temperature, and that the number of electrons that Cr can donate drops, although this is

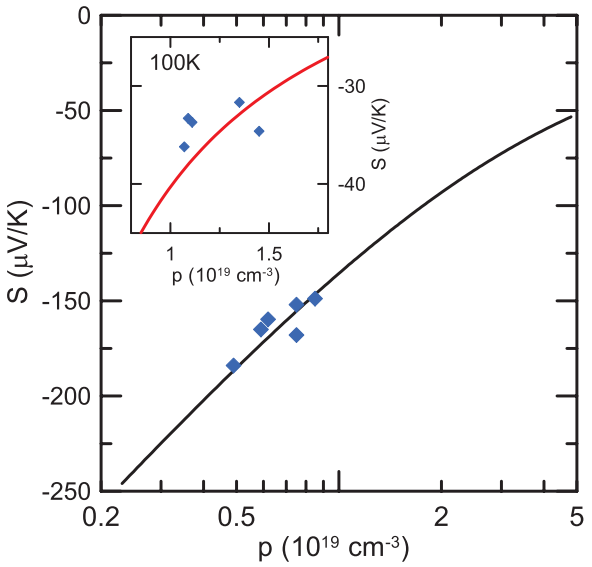

FIG. 3. (Color online) Pisarenko plot (Seebeck coefficient versus carrier concentration) for PbTe:Cr at 300 K and 100 K (inset). Solid lines are calculated for the conduction band of PbTe.

counteracted by the smearing of the Fermi surface. Note that this behavior of the Cr is identical to that of the In level in PbTe,[15] and that it has several consequences. First, like In, Cr is expected to act as a trap in PbTe at $T > 350$ K, shedding doubt on the results of Paul *et al.*,[6] as discussed in that footnote.[6] Second, since the movement between 80 and 350 to 400 K of the Cr or In levels vis-à-vis the conduction band edge mirrors half the change of the energy gap,[3] this implies that these levels have almost no T-dependence when referred to the middle of the gap at the L-point of the Brillouin zone. This suggests that, like the case for the In level, the physical origin of the dependence reported in Fig. 2 lies primarily in the T-dependence of the gap itself.

The scattering parameter (λ) is, within the experimental accuracy, constant for all samples and equal to that in Pb-rich PbTe,[16] indicating that the dominant scattering mechanisms involve acoustic and polar optical phonons, with no hint of resonant scattering.[3] The DOS-effective mass is not increased over the lowest conduction band of PbTe, as depicted by the dashed line. Indeed, Fig. 3 shows the Pisarenko relation between thermopower and carrier concentration (solid line) at $T = 300$ K, as calculated for the conduction band of PbTe.[17] Despite the doping level change of Cr and observed Fermi level pinning we do not see increased thermopower at any given carrier concentration, neither at 300 K nor at 100 K (see Fig. 3 inset).

IV. MAGNETISM

Doping of binary group IV tellurides with transition metals may form a dilute magnetic semiconductor (DMS)[18] when the solubility is sufficient. However, if the solubility of the transition metal in a particular telluride is low, second phases form that confuse the magnetic response, so that it is necessary to supplement magnetic measurements with others, such as transport and NMR studies in this work. Indeed, depending

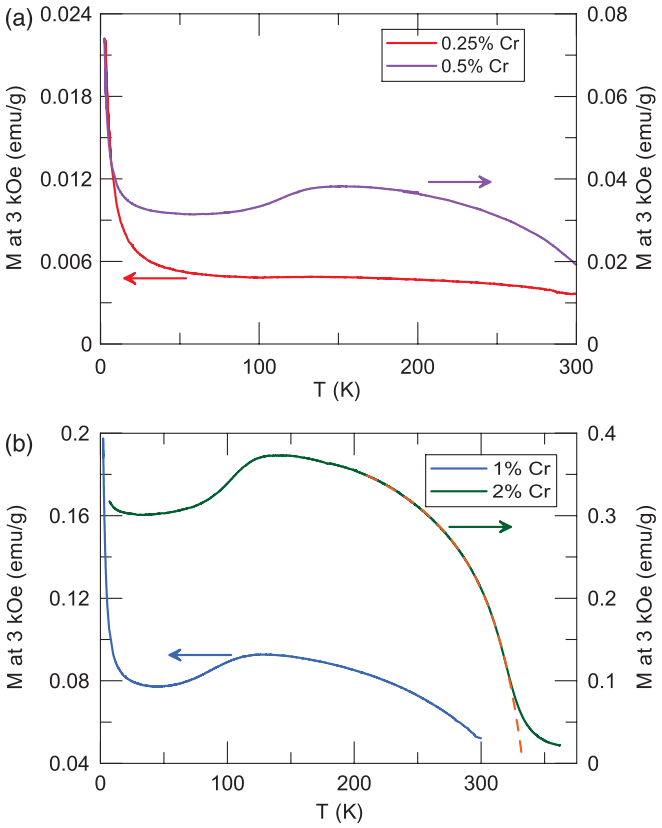

FIG. 4. (Color online) Temperature dependencies of the magnetization of PbTe doped with 0.25, 0.5, 1, and 2% Cr measured in a 3 kOe magnetic field. The dashed line is an order-parameter law fit to the data of the 2% Cr sample with a Curie temperature of $T_C \approx 335$ K.

on the properties of the second phase, parameters of the major phase measured in experiments can be inaccurate, e.g., the carrier concentration obtained from R_H or magnetization.[19] The following magnetic measurements of PbTe doped with Cr must be integrated with the other data to yield an understanding of the physical picture.

Figure 4 shows temperature dependencies of the magnetization of $Pb_{1-x}Cr_xTe$ doped with $x = 0.25\%$, 0.5%, 1%, and 2% (in atomic percent) of Cr measured in a 3 kOe magnetic field in a Quantum Design Physical Properties Measurement System's Vibrating Sample Magnetometer. Figure 5 shows their magnetization $M(H)$ measured versus magnetic field at various temperatures between 2.4 and 305 K and in magnetic fields up to 70 kOe. The raw data agree with those reported in Ref. 20 for $Pb_{1-x}Cr_xTe$ alloys measured in a 4 kOe magnetic field. The magnetization of all samples is positive and much larger than expected for diamagnetic PbTe,[21] which can be attributed to paramagnetic Cr ions embedded into the PbTe matrix or in other Cr-Te compounds.

Between 2.4 and 300 K, the magnetization curves of $Pb_{1-x}Cr_xTe$ samples show several features, which can be considered in three regions: (i) below ~30 K, (ii) at ~170 K, and (iii) around 305 K. The behavior of the magnetization at ~170 K can be attributed mostly to the presence of Cr_2Te_3, which exhibits ferromagnetic order below the Curie temperature $T_C = 170$ K.[22] However, Cr_2Te_3 has a complicated magnetic structure: its magnetization decreases with lowering of temperature, which can be associated with an increase of noncollinearity of Cr-magnetic moments[22] or due to antiparallel alignment of spins that belong to Cr_I, Cr_{II}, and Cr_{III} ions located on different sites.[23] The field-dependent magnetization of PbTe containing $x = 1\%$ and 2% Cr (Fig. 5) confirms the presence of the ferromagnetic phase at low temperatures; in addition it shows sharp saturation in low magnetic field, ~2 kOe, at 305 K. Because Cr_2Te_3 at 305 K is expected to be in the paramagnetic state,[22] we suggest that the observed saturated magnetization should be attributed to another more Cr-rich ferromagnetic phase. As there is a solid-solubility range to the Cr side of Cr_3Te_4 in the Cr-Te phase diagram, generating compounds with T_c between 317 K and 340 K,[24–26] we will label this composition $Cr_{3+\delta}Te_4$. An order-parameter fit with a T_c ~335 K fits the data for $x = 2\%$ well, as shown in Fig. 4. Finally, the presence of neither $Cr_{3+\delta}Te_4$ nor Cr_2Te_3 explains the increase below ~30 K, so the Curie-Weiss-like behavior of the magnetization of all four samples below ~30 K is attributed to paramagnetic Cr ions located on Pb sublattice (see NMR data) in the $Pb_{1-x}Cr_xTe$ solid solution. We do not see magnetic evidence for the presence of a minor Cr_5Te_8 phase, as the T_c of that compound varies between 180–230 K, depending on the exact Cr-Te ratio.[27]

The paramagnetic component attributable to the isolated Cr atoms in the PbTe lattice dominates both the T-dependence and the field dependence of the magnetization of the $x = 0.25\%$ Cr sample. In the temperature range $50 \leqslant T \leqslant 250$ K (Fig. 4) the moment is rather less T-dependent than a pure Curie-Weiss law, suggesting that even that sample has a minor amount of ferromagnetic phase present. Hence, the total magnetization of PbTe:0.25% Cr measured in experiment at 305 K can be shown as $M_{exp} = M_{par} + M_{dia} + M_{fer}$, where M_{par} contains contributions from paramagnetic Cr ions in $Pb_{1-x}Cr_xTe$ solid solution and from paramagnetic ions in Cr_2Te_3, which possesses paramagnetic properties above ~170 K.[22] As the ferromagnetic component of the magnetization attributable to $Cr_{3+\delta}Te_4$ in this $x = 0.25\%$ sample at 100 K to 300 K is small and constant in $H > 15$ kOe, M_{fer} can be subtracted first. The experimentally observed negative magnetization [Fig. 5(a)] is a result of the dominance of the diamagnetic component from the PbTe matrix. The diamagnetic susceptibility can be calculated next from the linear part of the magnetic field dependence of the magnetization at 305K to be $\chi_{dia} = M_{dia}/H = -2.4 \times 10^{-7}$ emu g^{-1} Oe^{-1}, smaller in absolute value than that measured for PbTe, $\chi_{dia} = -3.4 \times 10^{-7}$ emu g^{-1} Oe^{-1}.[21] The resulting $M_{par}(T)$ fits a $1/T$ dependence, with a paramagnetic susceptibility of $\chi_{par}/T = 1.46 \times 10^{-6}$ emu g^{-1} Oe^{-1} K^{-1}. After subtracting the field-dependent M_{dia} and M_{fer} from the 2 K and 15 K magnetization field sweeps, we fit the concentration N_{par-Cr} of paramagnetic Cr atoms to the experimental data with Brillouin functions (Fig. 5 inset) using $S = J = 2$, $L = 0$ for $3d^4$ Cr^{2+} with its orbital moment L quenched, which results in a net moment of 4.9 μ_B. The fit works well, confirming that the paramagnetic atoms are indeed Cr^{2+} and gives $N_{par-Cr} = 2.6 \times 10^{19}$ cm^{-3} (in mole fraction, $x_{par-Cr} = 0.19\%$), a value that is not significantly different from the concentration of free electrons in that sample below 50 K (Fig. 1). Simple electron counting rules do not explain the donor action of Cr^{2+} on the Pb sublattice (see NMR) of PbTe, and indeed the presence of Cr^{3+} has been postulated in the past,[18] but we suggest that

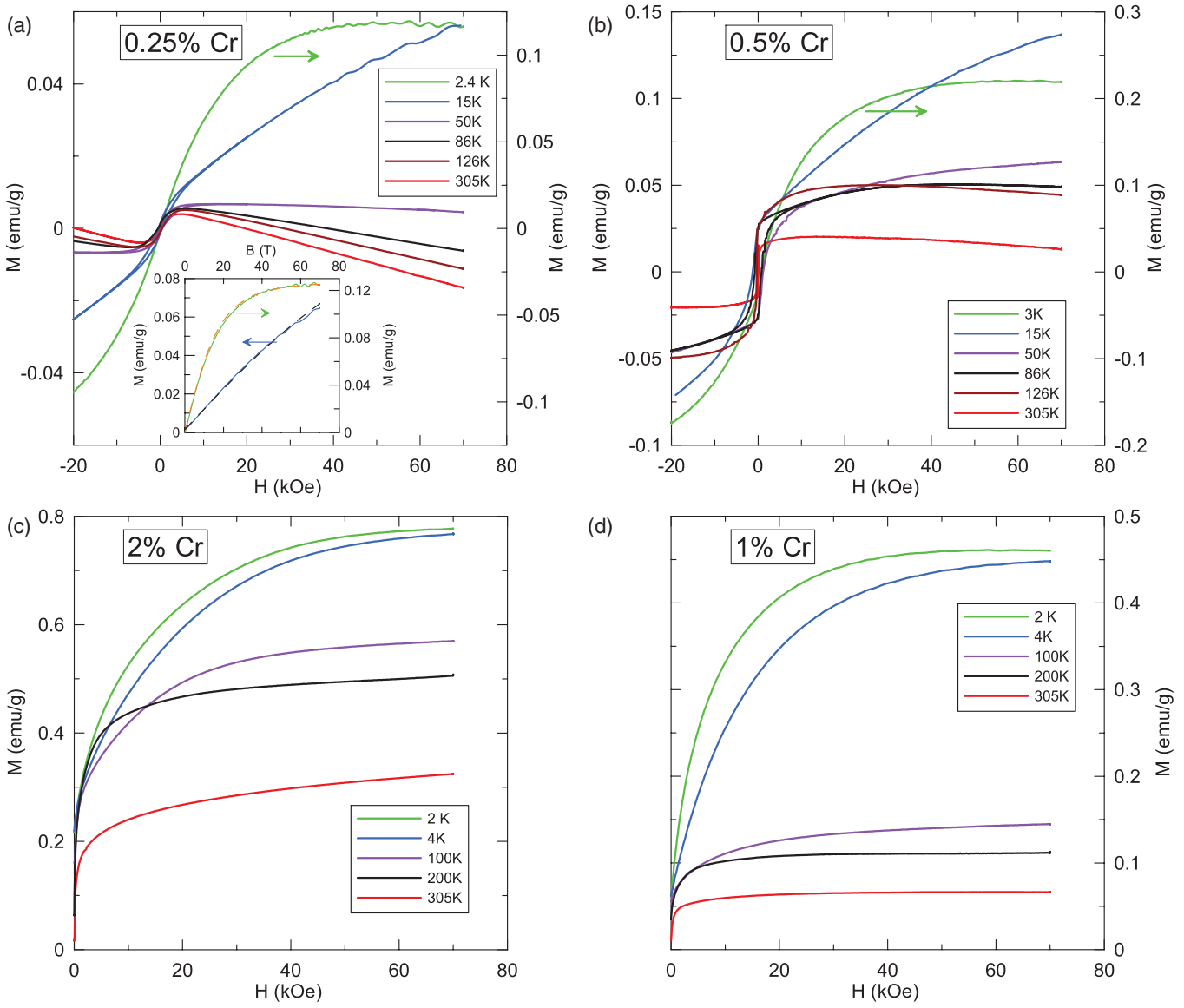

FIG. 5. (Color online) Magnetization of $Pb_{1-x}Cr_xTe$ doped with $x = 0.25$, 0.5, 1, and 2 at.% Cr measured at various temperatures in a magnetic field up to 70 kOe. The inset to the $x = 0.25\%$ frame shows as dashed lines Brillouin function fits to the magnetization assuming a $3d^4$ Cr^{2+} configuration using N_{par-Cr} as the only fitting parameter.

detailed band structure calculations are necessary to shed light on this point.

V. ^{125}Te NMR OF PbTe:Cr

The magnetic data shown previously are now complemented with ^{125}Te NMR data that will consolidate this view of PbTe:Cr as containing isolated Cr atoms as well as second phases, mostly $Cr_{3+\delta}Te_4$ and Cr_2Te_3. Such results are further consistent with Ref. 11, showing the presence of microinclusions in PbTe:{Sn,Cr} alloys. Given the possibility of an anomalous Hall effect in similar Cr chalcogenides (for example, $Sb_{2-x}Cr_xTe_3$)[28] the magnitude of the carrier concentration as determined from R_H will be confirmed here, although we sweep magnetic field to check for nonlinearities in Hall resistivity measurements. Finally, the presence of paramagnetic Cr ions and ferromagnetic phases in PbTe can induce paramagnetic effects[29] in ^{125}Te NMR peak position and relaxation times.

The ^{125}Te NMR spectra at 300 K in Fig. 6 exhibit distinct spectral peaks with shortened relaxation times that are not observed for PbTe doped (at similar concentrations) by elements without unpaired electrons.[30,31] The peak positions are consistent between samples, which shows that the additional peaks are not due to phases with very high charge-carrier concentration and large Knight shifts. The main peak of the PbTe matrix is observed near −1800 ppm, indicating a ∼+70-ppm Knight shift from the −1870 ppm chemical shift of PbTe.[30,31] This positive Knight shift indicates a moderately high n-type carrier concentration, consistent with the observed moderate T_1 relaxation time of ∼0.3 s that corresponds to a carrier concentration of $\sim 7 \times 10^{18}$ cm^{-3},[30] which is consistent with the carrier concentration measured by Hall effect at 300 K (see Fig. 1).

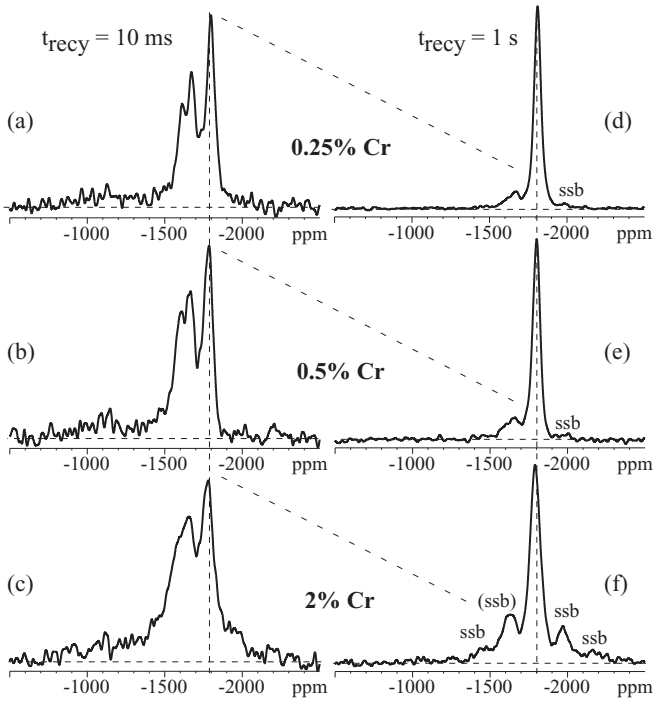

FIG. 6. ^{125}Te MAS NMR spectra of $Pb_{1-x}Cr_xTe$, for (top to bottom) $x = 0.25$, 0.5, and 2% Cr. Left column (a–c): Spectra after short recycle delay of 10 ms, highlighting signals of Te near Cr. Right column (d–f): Fully relaxed spectra. Spinning sidebands (labeled "ssb") spaced by $\nu_r = 22$ kHz from the main peak are prominent in part (f).

Interactions with the unpaired electrons of Cr can also lead to a frequency shift and reduction in T_1 due to both Fermi hyperfine and dipole-dipole couplings between unpaired Cr 3*d*-electrons and Te nuclear spins. This mechanism can slightly reduce the spin-lattice T_1 relaxation, and therefore the estimated carrier concentration, which is based on reference T_1 data from diamagnetic tellurides,[30] should be considered as an upper limit. The position of the PbTe-matrix peak shifts slightly with Cr content, indicating a slight (∼20%) increase in the carrier concentration from 0.25 to 2% Cr.

Two peaks are seen at ∼−1700 ppm, with shorter $T_1 \sim 10$ ms and $T_2 \sim 1$ ms and large noncubic local fields, which must all be attributed to the effect of Cr. These peaks can be observed quite selectively in spectra with short relaxation delays, which avoid overlap with the main peak at −1800 ppm (and its spinning sidebands). Together these peaks account for 8–12% of all Te in the three samples studied. This excludes their assignment to directly Cr-bonded Te, which accounts for only ∼1–2% of all Te. Instead, the intensity fraction is consistent with assignment to Te separated from Cr by three bonds (**Cr**-Te-Pb-**Te**). Since each Cr has 38 such Te second neighbors, their intensity is around 0.3% × 38 = 11%. The two peaks may correspond to different **Cr** ... **Te** bonding geometries, but details have not been determined.

In ^{125}Te NMR spectra of $Pb_{1-x}Cr_xTe$ acquired with more than 10^5 scans, consistently a small peak (∼1–2% of all Te) is detected at −1100 ppm, see Fig. 7. It is associated with very short $T_1 \sim 2$ ms and $T_2 \sim 0.12$ ms (compared to $T_1 = 300$ ms and $T_2 \sim 1.2$ ms for the PbTe-matrix signal), which

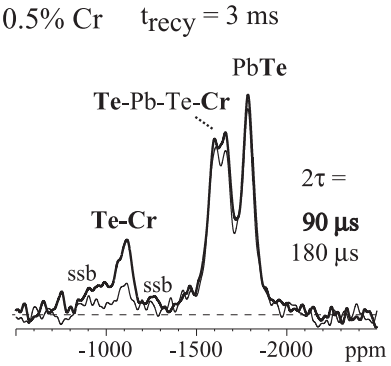

FIG. 7. ^{125}Te MAS NMR spectra of PbTe:0.5% Cr optimized for detection of the small signal at −1100 ppm by use of a short saturation-recovery delay of 3 ms and placement of the radio-frequency carrier at −1300 ppm. Thick line: Full spectrum after 90 μs of transverse relaxation (minimum delay). Thin line: Spectrum after 180 μs of transverse relaxation. The signal at −1100 ppm is strongly reduced due to a short transverse relaxation time. "ssb": Spinning sidebands.

tells us that this must be the signal of Te nearest to Cr, probably directly bonded (**Cr-Te**). The large (+700 ppm) frequency shift from −1800 ppm is probably mostly due to Fermi contact interaction between the unpaired electrons of Cr and the nuclear spin of ^{125}Te.

The intensities of Cr-induced peaks in Figs. 6(a)–6(c) and 6(d)–6(f) do not double from $x = 0.25\%$ to $x = 0.5\%$; they increase at most by a factor of 1.3. This indicates that the solubility of Cr in PbTe is low, i.e. $Pb_{1-x}Cr_xTe$ forms a solid solution only if $x \leqslant 0.4\%$. It does not increase much at $x = 2\%$ Cr; while the Cr-induced peaks are obscured by spinning sidebands in the fully relaxed spectrum, their intensity can be assessed well in the spectrum after 10-ms recycle delay [Fig. 6(c)]. At $x = 2\%$ Cr, the appearance of the spectra changes due to spinning sidebands induced by dipolar couplings to unpaired electrons of Cr. These are long-range effects of the ferromagnetic phases ($Cr_{3+\delta}Te_4$ and Cr_2Te_3) described previously.

VI. CONCLUSIONS

Cr forms a resonant donor level in the conduction band of PbTe, about 100 meV above the band edge at 0 K. Like the indium level, the Cr level moves into the gap as temperature reaches room temperature, probably due to the temperature dependence of the band gap itself. All studied PbTe:Cr samples contain paramagnetic Cr^{2+} ions on the Pb sublattice of $Pb_{1-x}Cr_xTe$ solid solution and a small fraction of ferromagnetic phases, most likely Cr_2Te_3 and $Cr_{3+\delta}Te_4$ with Curie temperature of 170 and 317 K, respectively. While it is not evident from simple electron counting rules how Cr^{2+} substituted for Pb^{2+} might act as a donor, ^{125}Te NMR shows signals from Te located in different local environments in the $Pb_{1-x}Cr_xTe$ solid solution: (i) in the PbTe matrix; (ii) next to Cr (Te-Cr); and (iii) separated from Cr by three bonds (Te-Pb-Te-Cr).

ACKNOWLEDGMENTS

Sample preparation, transport, and magnetic measurements at the Ohio State University were supported by ZT: Plus, Azusa, California and by the joint US National Science Foundation/Department of Energy Program on Thermoelectricity, NSF-CBET-1048622. The NMR work was supported by the US Department of Energy, Office of Basic Energy Sciences, Division of Materials Sciences and Engineering and performed at the Ames Laboratory, which is operated for the US Department of Energy by Iowa State University under Contract No. DE-AC02-07CH11358.

*Corresponding author: heremans.1@osu.edu

[1] J. P. Heremans, V. Jovovic, E. S. Toberer, A. Saramat, K. Kurosaki, A. Charoenphakdee, S. Yamanaka, and G. J. Snyder, Science **321**, 554 (2008).

[2] C. M. Jaworski, B. Wiendlocha, V. Jovovic, and J. P. Heremans, Energy and Environ. Sci. **4**, 4155 (2011).

[3] J. P. Heremans, B. Wiendlocha, and A. M. Chamoire, Energy Environ. Sci., doi: 10.1039/C1EE02612G (2011).

[4] K. Xiong, G. Lee, R. P. Gupta, W. Wang, B. E. Gnade, and K. Cho, J. Phys. D: Appl. Phys. **43**, 405403 (2010).

[5] C. M. Jaworski and J. P. Heremans, Phys. Rev. B **85**, 033204 (2012).

[6] B. Paul, P. K. Rawat, and P. Banerji, Appl. Phys. Lett. **98**, 262101 (2011). We prepared a double-doped PbTe:(Cr+I) sample with composition IV in this reference using our preparation technique and measured its thermopower and resistivity from 50 °C to 500 °C in an LSR-3 Linseis Seebeck and Resistivity unit. The thermopower increase and high power factor reported by Paul *et al.* are not reproduced. Instead the curves are monotonic extensions of Fig. 1, and in particular the resistivity increased with T to exceed 4 mΩ cm, consistently with the results in this article that Cr becomes a trap in PbTe above room temperature. The PbTe:(Cr+I) data are not further relevant to this article and are not reported.

[7] B. A. Akimov, P. V. Verteletskii, V. P. Zlomanov, L. I. Ryabova, O. I. Tananaeva, and N. A. Shirokova, Sov. Phys. Semicond. **24**, 848 (1990); B. A. Akimov, N. A. Lvova, and L. I. Ryabova, Phys. Rev. B **58**, 10430 (1998).

[8] M. I. Baleva and M. D. Borisova, J. Phys. C: Solid State Phys. **16**, L907 (1983); V. D. Vulchev and L. D. Borisova, Phys. Status Solidi A **99**, K53 (1987).

[9] V. D. Vulchev, L. D. Borisova, and S. K. Dimitrova, Phys. Status Solidi A **97**, K79 (1986).

[10] T. Story, Z. Wilamovski, E. Grodicka, B. Witkovska, and W. Dobrovolski, Acta Phys. Pol. A **84**, 773 (1993); E. Grodzicka, W. Dobrovolski, J. Kossut, T. Story, and B. Witkovska, J. Cryst. Growth **138**, 1034 (1994).

[11] E. P. Skipetrov, N. A. Pichugin, E. I. Slynko, and V. E. Slynko, Low Temp. Phys. **37**, 210 (2011).

[12] J. D. König, M. D. Nielsen, Yi-Bin Gao, M. Winkler, A. Jacquot, H. Böttner, and J. P. Heremans, Phys. Rev. B **84**, 205126 (2011).

[13] V. Jovovic and J. P. Heremans, Phys. Rev. B **77** 245204 (2008).

[14] J. P. Heremans, C. M. Thrush, and D. T. Morelli, Phys. Rev. B **70**, 115334 (2004).

[15] V. Jovovic, S. J. Thiagarajan, J. P. Heremans, T. Komissarova, D. Khokhlov, and A. Nicorici, J. Appl. Phys. **103**, 053710 (2008).

[16] J. P. Heremans, C. M. Thrush, and D. T. Morelli, J. Appl. Phys. **98** 063703 (2005).

[17] The Pisarenko relations for electrons and holes in PbTe are nearly identical, except for the sign of S, due to the symmetry in the conduction and valence bands at the L-point of Brillouin zone. This holds until $p \sim 5$–6×10^{19} cm^{-3}, where the lower valence band near the Σ-points begin to fill. There is no associated heavy conduction band involved in transport in PbTe.

[18] T. Story, in *Lead Chalcogenides, Physics and Applications*, edited by D. Khokhlov (Taylor and Francis Books, Inc., New York, 2003), Chap. 6, p. 385.

[19] E. M. Levin, X. W. Fang, S. L. Bud'ko, W. E. Straszheim, R. W. McCallum, and K. Schmidt-Rohr, Phys. Rev. B **77**, 054418 (2008).

[20] E. A. Zvereva, E. P. Skipetrov, O. A. Savelieva, N. A. Pichugin, A. E. Primenko, E. I. Slynko, and V. E. Slynko, J. Phys.: Conf. Series **200**, 062039 (2010).

[21] F. T. Hedgcock, P. C. Sullivan, and J. T. Grembowicz, Canadian J. Phys. **64**, 1345 (1986).

[22] J. Dijkstra, H. H. Weitering, C. F. van Bruggen, C. Haas, and R. A. de Groot, J. Phys.: Condens. Matter **1**, 9141 (1989).

[23] S. J. Youn, S. K. Kwon, and B. I. Min, J. Appl. Phys. **101**, 09G522 (2007).

[24] Y. Hinatsu, T. Tsuji, and K. Ishida, J. Solid State Chem. **120**, 49 (1995).

[25] N. Suzuki, T. Kanomata, R. Konno, T. Kaneko, H. Yamauchi, K. Koyama, H. Nojiri, Y. Yamaguchi, and M. Motokawa, J. Alloys Comp. **290**, 25 (1999).

[26] I. Stefaniuk, M. Bester, and M. Kuzma, Rev. Adv. Mater. Sci. **23**, 133 (2010).

[27] K. Lukoschus, S. Kraschinski, C. Näther, W. Bensch, and R. K. Kremer, J. Sol. State. Chem. **177**, 951 (2004).

[28] J. S. Dyck, C. Drasar, P. Lost'ak, and C. Uher, Phys. Rev. B **71**, 115214 (2005).

[29] J. D. Satterlee, Concepts in Magnetic Resonance **2**, 69 (1999).

[30] E. M. Levin, B. A. Cook, K. Ahn, M. G. Kanatzidis, and K. Schmidt-Rohr, Phys. Rev. B **80**, 115211 (2009).

[31] C. M. Jaworski, J. Tobola, E. M. Levin, K. Schmidt-Rohr, and J. P. Heremans, Phys. Rev. B **80**, 125208 (2009).